Inorganic Chemistry

Article

pubs.acs.org/IC

Oxorhenium(V) Complexes with Phenolate−Oxazoline Ligands: Influence of the Isomeric Form on the O-Atom-Transfer Reactivity

Jörg A. Schachner,[†] Belina Terfassa,[†,‡] Lydia M. Peschel,[†] Niklas Zwettler,[†] Ferdinand Belaj,[†] Pawel Cias,[§] Georg Gescheidt,[§] and Nadia C. Mösch-Zanetti*[,†]

[†]Institute of Chemistry, University of Graz, Schubertstrasse 1, 8010 Graz, Austria

[§]Institute of Physical and Theoretical Chemistry, Graz University of Technology, Stremayrgasse 9, 8010 Graz, Austria

Supporting Information

ABSTRACT: The bidentate phenolate−oxazoline ligands 2-(2′-hydroxyphenyl)-2-oxazoline (**1a**, Hoz) and 2-(4′,4′-dimethyl-3′,4′-dihydrooxazol-2′-yl)-phenol (**1b**, Hdmoz) were used to synthesize two sets of oxorhenium(V) complexes, namely, $[ReOCl_2(L)(PPh_3)]$ [L = oz (**2a**) and dmoz (**2b**)] and $[ReOX(L)_2]$ [X = Cl, L = oz (**3a** or **3a′**); X = Cl, L = dmoz (**3b**); X = OMe, L = dmoz (**4**)]. Complex **3a′** is a coordination isomer (*N*,*N*-cis isomer) with respect to the orientation of the phenolate−oxazoline ligands of the previously published complex **3a** (*N*,*N*-trans isomer). The reaction of **3a′** with silver triflate in acetonitrile led to the cationic compound $[ReO(oz)_2(NCCH_3)](OTf)$ ([**3a′**](OTf)). Compound **4** is a rarely observed isomer with a *trans*-O═Re−OMe unit. Complexes **3a**, **3a′**, [**3a′**](OTf), and **4** were tested as catalysts in the reduction of a perchlorate salt with an organic sulfide as the O acceptor and found to be active, in contrast to **2a** and **2b**. A comparison of the two isomeric complexes **3a** and **3a′** showed significant differences in activity: 87% **3a** vs 16% **3a′** sulfoxide yield. When complex [**3a′**](OTf) was used, the yield was 57%. Density functional theory calculations circumstantiate all of the proposed intermediates with *N*,*N*-trans configurations to be lower in energy compared to the respective compounds with *N*,*N*-cis configurations. Also, no interconversions between *N*,*N*-trans and *N*,*N*-cis configurations are predicted, which is in accordance with experimental data. This is interesting because it contradicts previous mechanistic views. Kinetic analyses determined by UV−vis spectroscopy on the rate-determining oxidation steps of **3a**, **3a′**, and [**3a′**](OTf) proved the *N*,*N*-cis complexes **3a′** and [**3a′**](OTf) to be slower by a factor of ∼4.

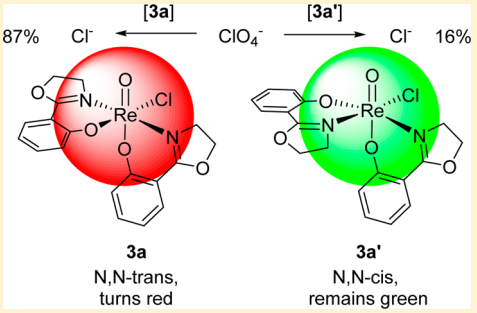

INTRODUCTION

The reduction of perchlorate under mild catalytic conditions is of general interest for application in wastewater treatment, where high levels of perchlorate potentially pose a risk to public health.[1−3] Even though perchlorate is a strong oxidizer, it is kinetically stable and therefore considered to be a nonlabile anion.[4] Because of their high chemical inertness and good solubility in both aqueous and organic media, the remediation of perchlorate salts in wastewater is challenging. Therefore, typical wastewater treatments using physical/chemical or biological techniques are hampered by significant disadvantages.[3,5] For these reasons, an effective procedure to chemically remove perchlorates would be highly favorable.

Few transition metals were found to chemically reduce perchlorate in stoichiometric reactions such as ruthenium(II), titanium(III), vanadium(II), and vanadium(III).[1] Complete perchlorate removal was accomplished in the presence of titanium(III) and *β*-alanine at near-neutral pH.[6] Molybdate was found to catalytically reduce perchlorate in the presence of stannous chloride as the O acceptor.[7] A molybdenum(IV) species was suggested as the active catalyst that is involved in an O-atom-transfer (OAT) mechanism with a single-step two-electron transfer. A further clear example of a two-electron process, as thoroughly elucidated by Espenson and co-workers, was found with the organometallic species methyltrioxorhenium ($MeReO_3$, MTO), where its reduced form, $MeReO_2$, reacts quickly in an OAT process with several substrates including perchlorate.[8]

Subsequently, in 2000 Abu-Omar and co-workers disclosed an oxorhenium(V) complex with phenolate−oxazoline ligands capable of catalytically reducing perchlorate in the presence of organic sulfides as O acceptors (Scheme 1).[9] On the basis of these rhenium complexes, also a heterogeneous version was developed using dihydrogen (H_2) as the electron donor in the reduction of perchlorate.[10]

Scheme 1. Rhenium-Catalyzed Reduction of Perchlorate

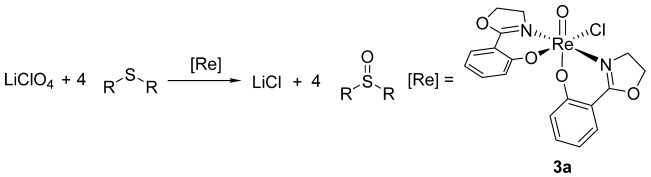

Received: August 7, 2014
Published: December 2, 2014

   dx.doi.org/10.1021/ic501932c | *Inorg. Chem.* 2014, 53, 12918−12928

Catalytic conditions of the homogeneous system were found to be mild because the reaction occurs at room temperature in CH_3CN/H_2O (95:5, v/v) with a high conversion rate with a catalyst loading of 3.2 mol %. Investigations of the mechanistic details of this unusual reaction including density functional theory (DFT) calculations were subsequently published.[11−14]

Within this publication, further insight into the catalytic reduction of perchlorate ions with the oxorhenium(V) complex **3a** is presented. Isolation of an isomeric form of **3a** allowed for a detailed comparative kinetic investigation. DFT calculations helped to unravel the influence of the geometric form on the catalytic activity in this important reaction.

RESULTS AND DISCUSSION

Synthesis of Ligands and Complexes. The oxazoline ligand **1a** (Hoz) was synthesized according to published procedures and ligand **1b** (Hdmoz) with slight modifications (Scheme 2).[15−17] In a general procedure, salicylic ester was condensed at high temperatures with the respective amino alcohol to give the corresponding carboxylic amide. Subsequent reaction with thionyl chloride resulted in ring closure to give the oxazoline ligands **1a** and **1b**.

Scheme 2. Synthesis of Published Phenoxide−Oxazoline Ligands 1a and 1b with Alternative One-Pot Synthesis of 1b

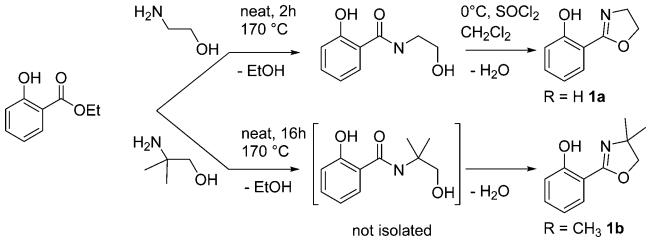

Ligand **1b**, however, can also be synthesized more conveniently in one step without isolation of the benzamide and use of thionyl chloride. When heated to 170 °C for 16 h with a Dean−Stark trap, the in situ formed carboxylic amide, which forms initially under elimination of EtOH, reacts further to give ring-closed product **1b** in 90−95% purity without use of thionyl chloride. If the same conditions are applied for the synthesis of **1a**, only traces of the ring-closed oxazoline can be observed.

Selective synthesis of monosubstituted complexes **2a** and **2b** was achieved with the precursor complex $[ReOCl_3(PPh_3)_2]$ via a protocol similar to that we published previously (Scheme 3).[18]

To a yellowish-green suspension of precursor $[ReOCl_3(PPh_3)_2]$[19] in acetonitrile was added **1a** or **1b**. Upon heating, a deep-green solution formed. After reflux for 2 h, the reaction was complete as determined by thin-layer chromatography [TLC; ethyl acetate/cyclohexane (1:1, v/v)]. Analytically pure **2a** and **2b** precipitated by cooling the reaction mixture to room temperature and could be isolated by filtration. NMR data for both complexes are consistent with those of a monosubstituted complex; the ^{31}P NMR resonance of the remaining PPh_3 ligand is at −18.1 ppm for **2a** and at −18.7 ppm for **2b** ($CDCl_3$). Crystals of **2a** suitable for single-crystal X-ray diffraction analysis were obtained by recrystallization from acetonitrile, as described in the Experimental Section.

Scheme 3. Synthesis of Complexes 2a and 2b

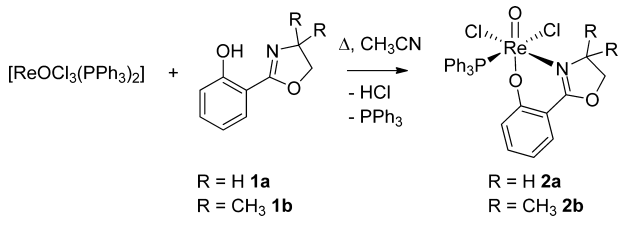

For disubstituted complexes of the type $[ReOX(L)_2]$, an octahedral complex coordinated by two bidentate ligands L and one monodentate ligand X, in principle a total of six isomers are conceivable (see Figure 1).[20] Two isomers originate from a symmetric coordination of the bidentate ligands (A and B) and the other four from an asymmetric coordination (C−F). Additionally, enantiomers exist for isomers B−F. In an asymmetric coordination (C−F), one bidentate ligand coordinates with both atoms in the equatorial plane and the other ligand in an equatorial−axial fashion. Most commonly for rhenium(V) complexes of this type, asymmetric isomers are observed, with the majority of the complexes belonging to types C and D.[20−22] In isomers C and D, the phenolate oxygen of the equatorial−axial ligand binds in the axial position trans to the terminal oxo ligand. If the two oxazoline moieties are trans to each other, this isomer is referred to as the *N,N*-trans isomer (C), with the other case being the *N,N*-cis isomer (D).

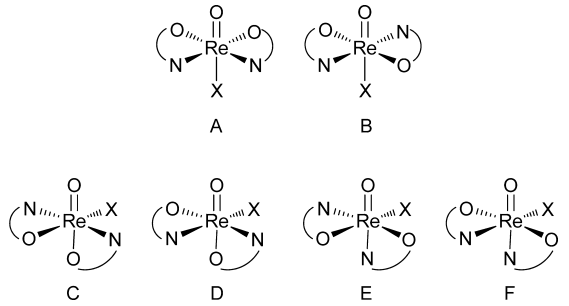

Figure 1. Possible isomers for octahedral oxorhenium(V) complexes bearing two bidentate and one monodentate ligand X.

For comparative reasons, we repeated the synthesis of compound **3a** according to the published procedure.[9] After isolation of **3a** from the reaction solution as described, we observed that the supernatant was still bright green, suggesting that some oxorhenium(V) product was still in solution. Upon concentration of the supernatant, more green material started to precipitate and was isolated. Characterization of the two materials (immediately precipitated and after concentration) showed them to be two distinct oxorhenium(V) complexes. Whereas the ^1H NMR spectrum of the former material (**3a**) was consistent with the published data,[9] the NMR data of the latter (**3a′**) exhibited two sets of ligand resonances pointing to another asymmetric isomer of the types C−F (Scheme 4; also see the Supporting Information, SI). Both isomers form in roughly the same amount, which is also reflected by the published yield of 49% for **3a**.[9] Complex **3a′** was isolated from the supernatant in 40% yield. Traces of **3a** can be removed from crude **3a′** via Soxhlet extraction with Et_2O, where **3a′** is less soluble than **3a**. We repeated the synthesis of complexes **3a**/**3a′** in two different solvents (e.g., MeOH, THF) and also from a different Re precursor (namely, $(NBu_4)[ReOCl_4]$) but found that the two isomers always formed in roughly equal

dx.doi.org/10.1021/ic501932c | Inorg. Chem. 2014, 53, 12918−12928

Scheme 4. Formation of Both Isomers of Previously Published[9] Complex 3a and New Complex 3a′ and Synthesis of Cationic Complex [3a′](OTf) in Acetonitrile

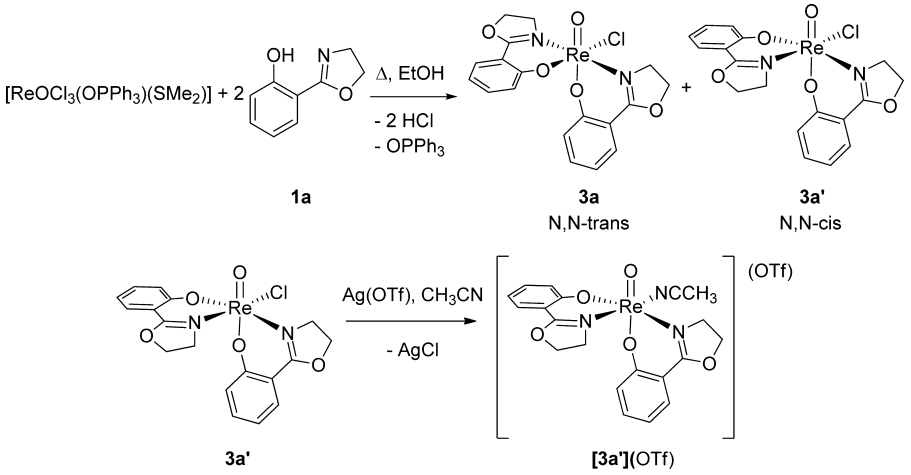

Scheme 5. Proposed Formation of Symmetric Complex 4

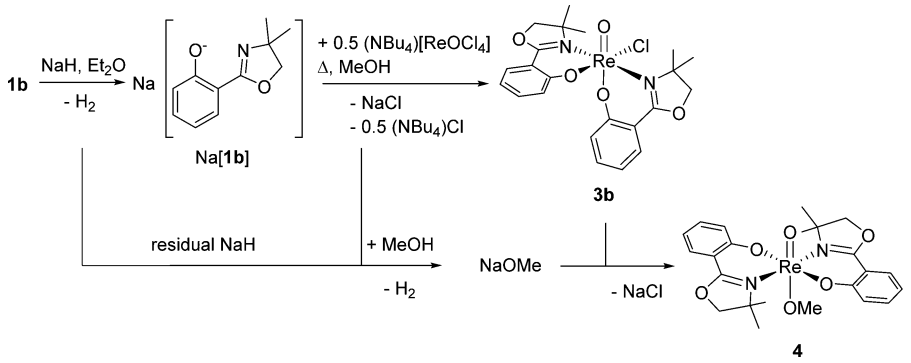

amounts. We were able to grow crystals of both fractions suitable for single-crystal X-ray diffraction analysis, confirming the nature of both isomers, namely, *N,N*-trans for **3a** (type C in Figure 1) and *N,N*-cis for **3a′** (type D in Figure 1). For kinetic investigations of perchlorate reduction (vide infra), the cationic complex [**3a′**](OTf) was synthesized and isolated by chloride abstraction with Ag(OTf) in acetonitrile (Scheme 4). Upon the addition of 1 equiv of Ag(OTf) to a green solution of **3a′**, an immediate precipitation of AgCl occurs. After filtration, analytically pure [**3a′**](OTf) can be isolated by the removal of solvent in high yield as a dark-green powder, which is slightly hygroscopic. Compound [**3a′**](OTf) is highly soluble in polar organic solvents. In the ^{1}H NMR spectrum, there are still two distinct sets of ligand signals observable, pointing to an asymmetric structure in solution. This can be rationalized by a vacant coordination site at the Re atom being coordinated by an acetonitrile solvent molecule even though it is not observed in the ^{1}H NMR spectrum because of a fast exchange with the deuterated solvent (CD_3CN).

Synthesis of the disubstituted complex employing the dimethyl-substituted ligand **1b** was carried out in analogy to **3a**. Starting from $[ReOCl_3(OPPh_3)(SMe_2)]$[23] and 2 equiv of **1b**, the reaction proceeds smoothly in refluxing ethanol. Upon cooling of the reaction mixture, a green precipitate of **3b** forms, which can be isolated by filtration. NMR data are consistent with formation of a disubstituted, phosphine-free complex. Two distinct sets of signals of the two ligand moieties in **3b** are observed, pointing to an asymmetric coordination environment. For example, four signals for the four methyl groups on the oxazoline moieties are observed in the ^{1}H NMR spectrum. Several attempts to grow single crystals and thereby determine the solid-state isomeric structure of **3b** have been unsuccessful so far. Nevertheless, it is highly feasible that the isolated material of **3b** is an asymmetric *N,N*-trans isomer of type C similar to **3a**. This assumption is mainly supported by two observations: first, the ^{1}H NMR spectrum in the aromatic region of **3b** is similar to that of **3a** but different from that of **3a′** (also see Figure S2 in the SI) and, second, complex **4**, which is obtained from a reaction of **3b** and NaOMe (Scheme 5), is found to be a symmetric *N,N*-trans isomer (type B in Figure 1), as determined by single-crystal X-ray diffraction analysis (vide infra). Furthermore, from a steric point of view, the *N,N*-trans isomer should adopt a more favorable orientation of the four methyl groups of the ligand moiety **1b**, being on opposite sides of the Re atom.

Compound **3b** can also be prepared by using the precursor $(NBu_4)[ReOCl_4]$. This required prior synthesis of the sodium salt of **1b** by reacting it with NaH (60% dispersion in mineral oil) in diethyl ether. The resulting precipitate Na(**1b**) was washed with hexane and used directly in a subsequent reaction with $(NBu_4)[ReOCl_4]$ in methanol (Scheme 5). Upon characterization of the crude reaction mixture by ^{1}H NMR spectroscopy, we observed in some experiments, besides the expected signals for **3b**, a second set of resonances (5−10%) that were consistent with a symmetric isomer of an oxorhenium(V) complex (type A or B in Figure 1). This new

dx.doi.org/10.1021/ic501932c | *Inorg. Chem.* 2014, 53, 12918−12928

compound **4** was more soluble in MeOH than **3b** and could therefore be separated from **3b** via filtration. The ^{1}H and ^{13}C NMR spectra of **4** displayed only one set of ligand resonances, indicating formation of a symmetric complex (type A or B in Figure 1). In addition, a new signal integrating for three protons was observed at 3.37 ppm in the ^{1}H NMR spectrum ($CDCl_3$). The acquired MS spectrum was consistent with formation of a disubstituted complex of the general formula $[ReO(X)(L)_2]$ without a chloro ligand based on the mass fragments and isotope patterns. Instead, the anionic ligand X in **4** could be identified as a methoxy ligand, explaining the new signal in the ^{1}H NMR spectrum. A single-crystal X-ray diffraction analysis unequivocally revealed complex **4** to be the symmetric isomer of type B (Figure 1) with the formula $[ReO(OMe)(dmoz)_2]$.

It is feasible that excess NaH from the deprotonation step of ligand **1b** is carried over to the second step of complex formation. There, excess NaH can react with the solvent MeOH, forming NaOMe, and subsequently the chloro ligand in **3b** is substituted by a methoxy ligand in a salt metathesis reaction. If extra care is taken to remove all excess NaH from ligand deprotonation, only **3b** is obtained. Also, when **3b** is dissolved in MeOH and NaH is added, the formation of **4** can be observed, albeit only in small yields. When 1 equiv of NaOMe is reacted with **3b**, the reaction proceeds smoothly to give **4** in good yield (see the Experimental Section). Probably because of steric repulsion of the methyl groups on the oxazoline moiety, the symmetric *N*,*N*-trans configuration is adopted (type B in Figure 1). Very recently, a similar pathway for formation of such a symmetric methoxy complexes was reported.[24]

Molecular Structures of Compounds 2a, 3a′, and 4. The molecular structures, determined by single-crystal X-ray diffraction analyses, are displayed in Figures 2 (**2a**), 3 (**3a** and **3a′**), and 4 (**4**). Selected details on data collection and structure refinement for all four complexes can be found in Table 2; selected bond lengths and angles as well as full details on the data collection and structure refinements for each complex separately can also be found in the SI.

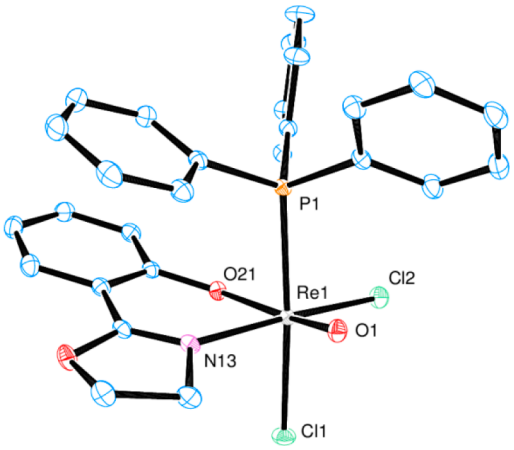

Figure 2. Molecular views (50% probability level) of complex **2a** (H atoms are omitted for clarity).

Single crystals of complex **2a** were obtained by crystallization in acetonitrile at room temperature. Complex **2a** adopts a distorted octahedral geometry around the Re center. The trans coordination of the phenolate O atom to the oxo ligand is well documented in the literature.[19,25] All bond angles and distances fall within the expected range for similar complexes of the type $[ReOCl_2(L)(PPh_3)]$.[18,22,26,27] In complex **2a**, the Re1═O1 bond distance is 1.6868(16) Å, which is in the typical range for such bonds (1.688−1.694 Å). The Re1−Cl1 bond distance is 2.4020(4) Å, which is longer than the Re1−Cl2 bond distance, 2.3692(4) Å, reflecting the trans influence of PPh_3 ligands. The angle between the trans oxo and phenolate O atom, O1−Re1−O21, is 166.06(7)° and severely deviates from 180° for an ideal octahedral structure.

Single crystals of **3a** as well as **3a′** were obtained by recrystallization from dichloromethane/pentane at −25 °C. Because the crystal structure of **3a** was not published in the original paper of Abu-Omar et al.,[9] it is discussed here together with the new structure of **3a′**. A comparison of selected bond lengths and angles is given in Table 1.

Crystallographic analysis of the molecular structure of **3a′** displays a disubstituted complex, adopting the asymmetric *N*,*N*-cis configuration (for a structural discussion of **3a**, refer to the SI). As displayed in Figure 3, the Re center is surrounded in a distorted octahedral fashion by two oxazoline moieties, a terminal oxo and a chloro ligand. The oxazoline ligands bind in an asymmetric fashion to the Re atom (type D in Figure 1), with the oxazoline N atoms arranged cis to each other (*N*,*N*-cis). Again the measured bond distances and angles are within the expected range for oxorhenium(V) complexes of the type $[ReOCl(L)_2]$.[20,22,28−30] The Re1═O1 bond in **3a′** shows a distance of 1.689(8) Å and the Re1−Cl1 bond of 2.383(3) Å. Both phenolate O atoms show a distance very similar to the Re atom at Re1−O21 of 1.999(7) Å and Re1−O41 of 1.983(7) Å. The bonding distances between the two oxazoline N atoms and the Re center in **3a′** are virtually the same [Re1−N13 at 2.117(9) Å and Re1−N33 at 2.116(10) Å]. Distortion from the octahedral geometry (180°) in **3a′** is visible, for example, in the trans bond angle O1−Re1−O21, which is 166.4(4)°. In general, the majority of fully characterized oxorhenium(V) complexes adopt the asymmetric coordination of type C or D (Figure 1), and both *N*,*N*-cis and *N*,*N*-trans complexes have been described in the literature. Three closely related phenolate−oxazoline oxorhenium(V) complexes and a cationic oxoimidorhenium(VII) complex were fully characterized and published previously.[30−32] All three adopt the isomeric *N*,*N*-trans form in the solid state as **3a**. In contrast, the phenolate−thiazoline complex adopts the isomeric *N*,*N*-cis form also displayed by **3a′**.[12,14] A comparison of the bond distances in **3a** and **3a′** around the Re center generally shows only slight differences despite their different geometries. The Re1−O1 and Re1−O21 distances, both being trans to each other in **3a** as well as in **3a′**, are virtually identical. The other distances of the bonds, where their trans ligand changes, are slightly different, e.g., with the Re1−Cl1 bond distance in **3a′** being 2.383(3) Å and that in **3a** 2.4093(10) Å. Although this difference is close to a standard deviation of 3σ, the trend is, in principle, in accordance with a stronger trans influence by the anionic phenolate O atom O41 in **3a** versus the neutral oxazoline N atom N33 in **3a′**, elongating the Re1−Cl1 bond in the former. It is interesting to note that, in the initial first two publications from 2000 and 2001 by Abu-Omar et al., complex **3a** was correctly predicted to be the *N*,*N*-trans isomer.[9,11] From 2003 onward, however, all of the mechanistic investigations were based on the assumption of complex **3a** being the *N*,*N*-cis isomer,[12,14] which we are convinced, on the basis of the results presented here, represents an incorrect assumption.

dx.doi.org/10.1021/ic501932c | *Inorg. Chem.* 2014, 53, 12918−12928

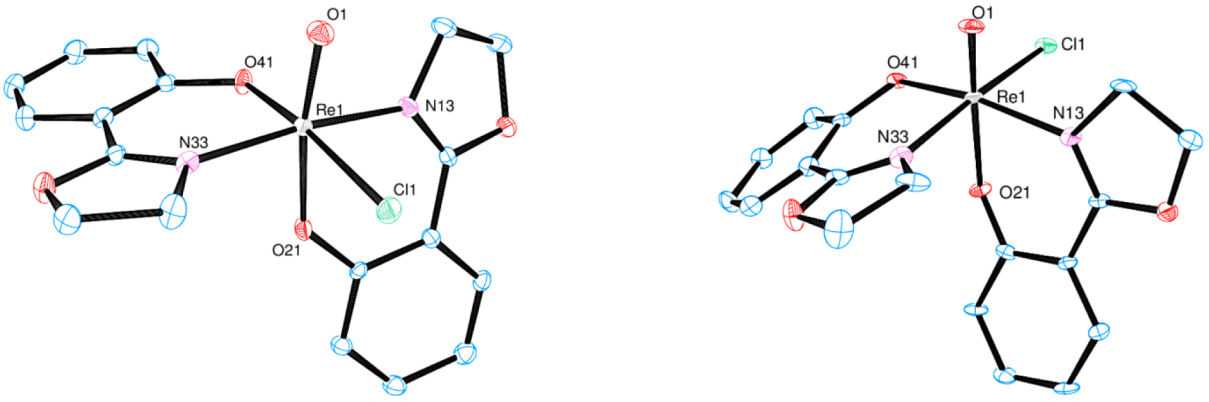

Figure 3. Molecular views (50% probability level) of complex **3a** (left, *N*,*N*-trans isomer) and **3a′** (right, *N*,*N*-cis isomer; H atoms omitted for clarity).

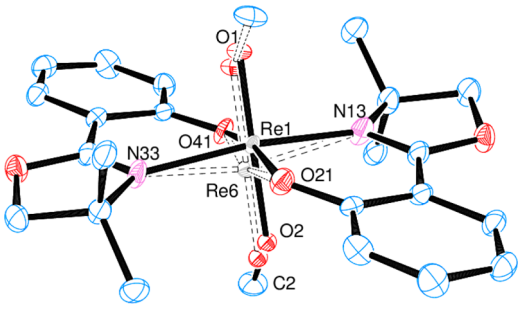

Figure 4. Molecular view (50% probability level) of complex **4** (H atoms omitted for clarity). Bonds connecting disordered atoms with lower occupation factors are drawn with dashed lines.

Table 1. Comparison of Bond Distances [Å] in 3a and 3a′

	3a	3a′
Re1═O1	1.692(3)	1.689(8)
Re1−O21	2.001(3)	1.999(7)
Re1−O41	2.007(3)	1.983(7)
Re1−N13	2.112(2)	2.117(9)
Re1−N33	2.064(3)	2.116(10)
Re1−Cl1	2.4093(10)	2.383(3)

X-ray crystallographic data collection for **4** found two disordered molecules in the unit cell partially overlapping each other. Two Re centers (Re1 and Re6) occupy slightly different positions in the crystal lattice. The refinement resulted in two quite different site occupation factors summing to 1 [Re1 = 0.688(2) and Re6 = 0.312(2)], which means that 68.8% of the Re atoms in the crystal lattice occupy similar positions and the remaining 31.2% of the Re atoms are located on the other position. Also the oxo and methoxy ligands bonded to Re6 are in the opposite configuration and overlap with the oxo and methoxy ligands bonded to Re1.

For the structural discussion of **4**, only the structure containing Re1 is considered. The Re center in **4** is coordinated in a distorted octahedral fashion by two N and two O atoms from the ligand moieties, all in the equatorial plane, and a terminal oxo and a methoxy ligand in the axial positions. The terminal oxo ligand O1 is located at a distance of 1.715(6) Å, and O2 of the methoxy ligand trans to O1 is at 1.890(4) Å to Re1. The two oxazoline ligands also show a distorted coordination to Re1, reflected in the slightly different bond distances of both the N and O atoms to Re [Re1−N13 2.073(2) Å, Re1−N33 2.155(2) Å; Re1−O21 1.973(2) Å, Re1−O41 2.105(2) Å].

Crystallographically characterized symmetric oxorhenium(V) complexes like **4** with a *trans*-O═Re−OMe core are rather scarce in the literature.[20−22,29,32,33] Another type of symmetric complex is formed upon reaction of **3a** with Ag(OTf) in acetonitrile. The molecular structure was found to be the symmetric cationic complex $[ReO(oz)_2(H_2O)](OTf)$ ([**3a**]-(OTf); type B in Figure 1) with a *trans*-O═Re−OH_2 moiety (Scheme 6).[11] This is in contrast to **3a′**, where after reaction with Ag(OTf) in acetonitrile an asymmetric compound with an acetonitrile molecule cis to oxo is formed, as evidenced by ^{1}H NMR spectroscopy (two sets of ligands) as described above. This is consistent with a previous observation where the *N*,*N*-cis complex $[ReOCl(pyz)_2]$ [Hpyz = 3-(2-hydroxyphenyl)-1-methyl-1*H*-pyrazole] upon the addition of Ag(OTf) in acetonitrile reacted to the cationic complex $[ReO(pyz)_2(CH_3CN)](OTf)$ with an asymmetric configuration.[18]

Closer inspection of the variable-temperature (VT)-NMR experiment of compound [**3a**](OTf), as reported previously,[14] shows behavior very similar to that of our previous results with $[ReOCl(pyz)_2]$.[18] We have assigned our VT-NMR data to a dynamic behavior in solution under retention of the asymmetric structure. The exact 1:1 ratio of all protons at low temperature gave good evidence for equilibrium of two asymmetric isomers. Similarly, in the reported VT-NMR spectrum of [**3a**](OTf), also a 1:1 ratio of all protons is observed at low temperature. However, the authors explain this observation by equilibrium between a symmetric rhenium complex with a molecule of acetonitrile coordinated and the respective complex without a solvent molecule coordinated. Considering that acetonitrile is the NMR solvent and therefore present in large excess, we find this explanation rather unlikely because it would require an equilibrium constant of exactly $K = 1$ at low temperature (exactly half of the complex is coordinated by acetonitrile and the other half is not to give the observed 1:1 ratio of proton signals). It is thus feasible that in an acetonitrile solution also compound [**3a**](OTf) does not isomerize but rather retains it asymmetric nature. This is important in view of the OAT reactivity and its mechanistic implications.

Perchlorate Reduction. The transfer of an O atom from perchlorate to diphenyl sulfide using the newly synthesized oxorhenium(V) complexes according to Scheme 1 was investigated. For comparative reasons, reaction conditions identical with those reported by Abu-Omar and co-workers were employed.[9] Thus, the perchlorate reduction reactions

dx.doi.org/10.1021/ic501932c | *Inorg. Chem.* 2014, 53, 12918−12928

Table 2. Selected Details on Crystallographic Data and Structure Refinement for 2a, 3a, 3a′, and 4

	2a	3a	3a′	4
cryst description	plate, green	plate, green	needle, green	plate, green
cryst size (mm)	0.32 × 0.26 × 0.20	0.28 × 0.22 × 0.14	0.11 × 0.10 × 0.05	0.26 × 0.24 × 0.16
cryst syst, space group	triclinic, $P\bar{1}$	monoclinic, $P2_1/c$	monoclinic, $P2_1/n$	monoclinic, **Cc**
unit cell dimens				
a (Å)	9.7861(5)	9.3096(5)	7.3979(5)	17.8638(6)
b (Å)	10.0085(5)	7.9506(4)	25.1497(16)	8.6385(3)
c (Å)	13.7063(7)	23.3508(11)	9.5588(6)	14.9031(5)
α (deg)	74.919(2)	95.817(2)	90.331(3)	111.1760(10)
β (deg)	75.716(2)			
γ (deg)	75.064(2)			
reflns colld/unique	25345/8703	23110/5003	15603/4655	11240/5874
sign unique reflns [$I > 2\sigma(I)$]	8253	4760	4107	5779
R(int), $R(\sigma)$	0.0217, 0.0219	0.0265, 0.0216	0.0882, 0.0796	0.0194, 0.0243
completeness to θ (%)	30.0° = 99.6	30.0° = 99.9	29.0° = 98.8	30.0° = 99.9
refinement method	full-matrix least squares on F^2			
data/parameters/restraints	8703/380/0	5003/248/0	4655/248/1	5874/330/2
GOF on F^2	1.065	1.394	1.115	1.072
final R indices [$I > 2\sigma(I)$]	R1 = 0.0192, wR2 = 0.0480	R1 = 0.0334, wR2 = 0.0650	R1 = 0.0653, wR2 = 0.1578	R1 = 0.0172, wR2 = 0.0444
R indices (all data)	R1 = 0.0202, wR2 = 0.0485	R1 = 0.0358, wR2 = 0.0656	R1 = 0.0784, wR2 = 0.1634	R1 = 0.0181, wR2 = 0.0451

Scheme 6. Formation of Different Isomers of Cationic Oxorhenium(V) Complexes

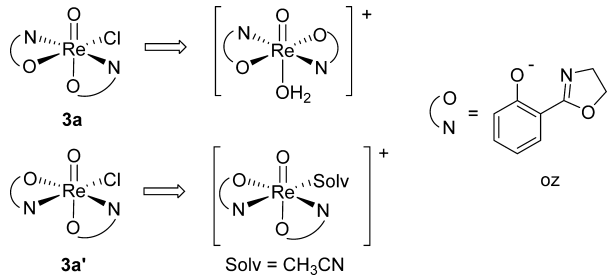

were performed in CD_3CN/D_2O (95:5, v/v) with 3.2 mol % catalyst loading using either $LiClO_4$ or $AgClO_4$ and 4 equiv of diphenyl sulfide at room temperature. All experiments were repeated at least four times, giving error margins of ±5%. The reaction progress was monitored by ^{1}H NMR spectroscopy via integration of the resonances of formed Ph_2SO. Data are given in Table 3.

Table 3. Yields of Diphenyl Sulfoxide[a]

	3a	3a′	3a′	3a′	3a′	[3a′](OTf)	4	2a, 2b
conversion after 7 h [%]	87[b]	16	30[c]	32[d]	40[e]	57	9	0

[a]Conditions: 3.2 mol % catalyst, CD_3CN/D_2O (95:5, v/v), 20 °C. [b]Previously reported.[9] [c]Reaction temperature 50 °C. [d]Reaction time 24 h. [e]$AgClO_4$ was used instead of $LiClO_4$.

Conversion of $LiClO_4$ to LiCl, as indicated by the yield of sulfoxide, with **3a** reaches 87% after 7 h at 20 °C when Ph_2S was used as the O acceptor.[9] In contrast, the cis isomer **3a′** yields only 16% under the same conditions. Longer reaction time increased the yield of sulfoxide to 32% after 24 h. When heated to 50 °C, a yield of sulfoxide of 30% with **3a′** was reached after 7 h. Furthermore, upon prior abstraction of the Cl atom from the Re center by employing the cationic complex [**3a′**](OTf), the perchlorate reduction activity increased significantly, giving a 57% yield of sulfoxide after 7 h. Also, the in situ generated cationic compound from **3a′** by using $AgClO_4$ instead of $LiClO_4$ gave slightly better yields than the standard reaction (40% conversion of Ph_2S after 7 h). To complete the picture, we also tested the monosubstituted compound. In contrast, complexes **2a** and **2b** were found to be inactive under any condition. Instead, the initially green reaction mixtures turned colorless, pointing to the formation of catalytically inactive rhenium(VII) species.

An interesting observation is the different color change after the addition of $LiClO_4$ to **3a** and **3a′**, respectively: while **3a** turns from green (λ_{max} = 654 nm) to red (λ_{max} = 530 nm),[9] **3a′** remains green (λ_{max} = 641 nm). However, when $AgClO_4$ was added to a solution of **3a′** in CH_3CN/H_2O (95:5, v/v), the color of the reaction mixture turned red (λ_{max} = 437 nm) immediately. A similar color change was observed for [**3a′**](OTf); the initial dark-green reaction solution (λ_{max} = 582 nm) turned red (λ_{max} = 520 nm) immediately after the addition of $LiClO_4$.

Scheme 7. Initial Steps in the Proposed Catalytic Cycle of Perchlorate Reduction Catalyzed by 3a[12,14] (IP = Intermediate Product; Int = Intermediate)

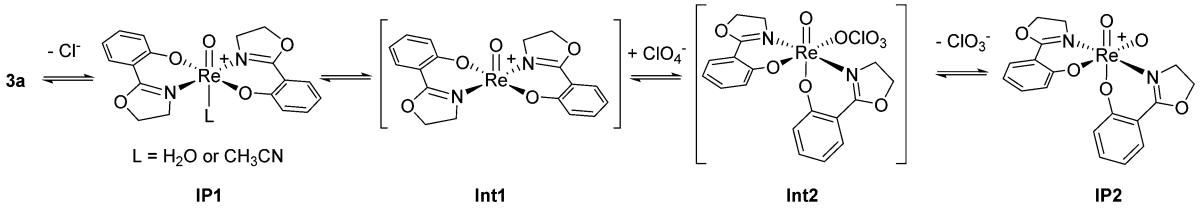

dx.doi.org/10.1021/ic501932c | Inorg. Chem. 2014, 53, 12918−12928

The initial steps of the catalytic cycle involving **3a**, as proposed by Abu-Omar and co-workers, are shown in Scheme 7.[12,14] The occurrence of the red color was assigned to formation of the oxidized, cationic dioxorhenium(VII) intermediate product **IP2**. The first three steps in the proposed cycle are described to be accompanied by several isomeric complex rearrangements. Starting from **3a** (asymmetric isomer type C in Figure 1), chloride abstraction leads to intermediate product **IP1** (symmetric type B). The loss of solvent molecule S from **IP1** leads to coordinative unsaturated intermediate **Int1**. This intermediate can then accept a substrate molecule of perchlorate under concomitant isomeric rearrangement to **Int2** (asymmetric type D). The rate-determining step (RDS) is proposed to be the oxidation of **Int2**, leading to the cationic dioxorhenium(VII) species **IP2**.

We find the proposed cycle interesting and intriguing. If **IP2** corresponds indeed to the *N*,*N*-cis isomer, it is remarkable that our preformed *N*,*N*-cis isomer seems to be converted to **IP2** to a significantly lower extent, as evidenced by the fact that compound **3a′** shows no color change from green to red upon the addition of $LiClO_4$ under catalytic conditions. This indicates that the formation of **IP2** occurs to a significantly lower extent because some catalytic activity is still observed. Although after chloride abstraction (by using $AgClO_4$ or [**3a′**](OTf)) the red color is observable, catalytic yields are still lower compared to those of **3a**. Thus, removal of the Cl ligand activates the system. The oxidation of **3a′** to a dioxo intermediate (presumably **IP2**) is hindered compared to the active isomer **3a** because of a higher energy barrier for removal of the Cl in **3a′**. However, this cannot be the only reason because catalytic yields are still lower after removal of the Cl. This points to two different dioxo intermediates with **3a** and **3a′**, respectively. Thus, it seems likely that the overall configuration remains the same throughout the catalytic cycle (**3a** remains *N*,*N*-trans and **3a′** *N*,*N*-cis), which is in contrast to the previously proposed cycle (Scheme 7).[12,14] In **3a′**, a neutral oxazoline N atom is located trans to the chloro ligand and, in **3a**, an anionic phenolate O atom. The lower trans effect and influence of the neutral N versus the anionic O ligand leads both to the higher energy for Cl removal and to a lowered catalytic activity throughout the cycle.

The following section describes DFT calculations of the initial removal of the Cl ion for both isomers.

Theoretical Investigations. The molecular background for rationalizing the lower reactivity of **3a′** compared with **3a** is provided by calculating the Gibbs free energies for the intermediates for both isomers (calculated complexes are presented in curly brackets to avoid confusion with isolated complexes). It has been shown that calculations based on the B3LYP 6-31+G(d)[34−36] functional with the ECP LANL2DZ basis set[37−39] yield data matching experimental results for related complexes;[27,32,40−42] accordingly, we have used this protocol for our calculations. The crystal structures of **3a** and **3a′** were taken as the starting geometries for the calculations, and indeed optimization does not substantially alter the experimental values (also see Table S1 in the SI). To obtain a clear-cut distinction between **3a** and **3a′**, we have solely computed the energy profile for removal of the Cl anion by scanning the potential energy surface. The Re−Cl bond was elongated in 0.15 Å steps, while for each distance, the geometry was optimized (relaxed geometry). In Figure 5, the corresponding potential energies are displayed.

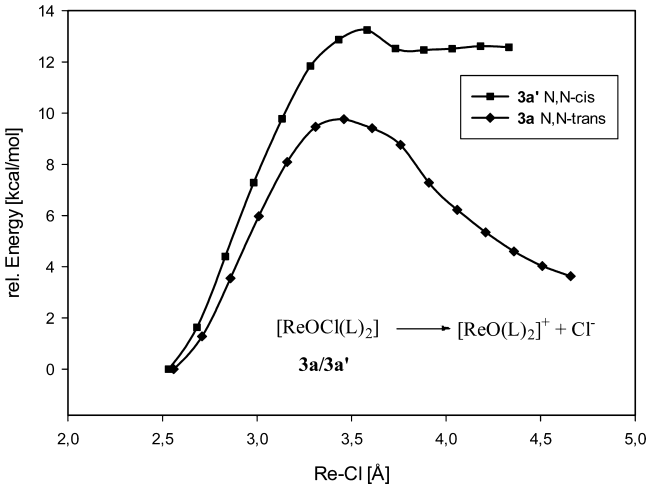

Figure 5. Calculated relative potential energies for Cl removal from {**3a**} and {**3a′**} calculated by DFT at the B3LYP level of theory (see Computational Details for basis set assignments).

Although this model does not account for the overall energy hypersurface of the entire reaction, it is well suited to clearly indicate that the energy required to remove the Cl is higher (ca. 3−4 kcal/mol) for the *N*,*N*-cis isomer **3a′** than for the *N*,*N*-trans isomer **3a**, i.e. transfer of the Cl preferably proceeds from **3a**. The transition state structures of complexes {**3a-TS1**} and {**3a′-TS1**} are shown in Figure 6.

The cationic five-coordinated complexes $\{\mathbf{3a}\}^+$ and $\{\mathbf{3a'}\}^+$ (for the calculated structures, refer to the SI) after chloride abstraction adopt a slightly distorted square-pyramidal coordination geometry and retain their parent configurations, *N*,*N*-trans in $\{\mathbf{3a}\}^+$ and *N*,*N*-cis in $\{\mathbf{3a'}\}^+$. Again $\{\mathbf{3a}\}^+$ is more stable (9.6 kcal/mol) than $\{\mathbf{3a'}\}^+$. This finding is in contrast to the previously suggested mechanism.[14]

The RDS of perchlorate reduction by $\{\mathbf{3a}\}^+$ and $\{\mathbf{3a'}\}^+$ is proposed to be cleavage of the perchlorate anion, forming the rhenium dioxo species (Scheme 7). To attain the corresponding transition states, the ion pairs of $\{\mathbf{3a}\}^+$ and $\{\mathbf{3a'}\}^+$ with the perchlorate anion were calculated, and then the corresponding transition states **TS2** were computed. Finally, the optimized geometries for both intermediate oxidized complexes ({**3a-OClO$_3$**} and {**3a′-OClO$_3$**}) after perchlorate reduction were determined (Figure 7).

The coordination of perchlorate proceeds significantly easier for the *N*,*N*-trans isomer $\{\mathbf{3a}\}^+$ than for $\{\mathbf{3a'}\}^+$, as can be anticipated from the transition state energies of 2.9 vs 12.8 kcal/mol, respectively (Figure 8). The Gibbs free energies of the products also indicate the preference of the $\{\mathbf{3a}\}^+$ isomer over $\{\mathbf{3a'}\}^+$ (38.3 vs 22.4 kcal/mol). It is furthermore significant that the optimized geometries of the oxidized complexes differ. For the *N*,*N*-trans isomer {**3a-OClO$_3$**}, a complete Cl−O bond scission is observed, resulting in the fully oxidized rhenium(VII) dioxo complex and a chlorate anion. In contrast, for the *N*,*N*-cis isomer {**3a′-OClO$_3$**}, the minimum structure reveals no cleavage, with the perchlorate anion still being coordinated to the Re atom, with an elongated Cl−O bond of 2.53 Å. This is consistent with the overall slower kinetics observed for the cis isomer **3a′**.

Kinetic Investigations. As described above, both complexes displaying the *N*,*N*-cis isomeric forms **3a′** and [**3a′**](OTf) showed lower catalytic activity compared to the *N*,*N*-trans complex **3a**. In order to obtain additional insight into

dx.doi.org/10.1021/ic501932c | *Inorg. Chem.* 2014, 53, 12918−12928

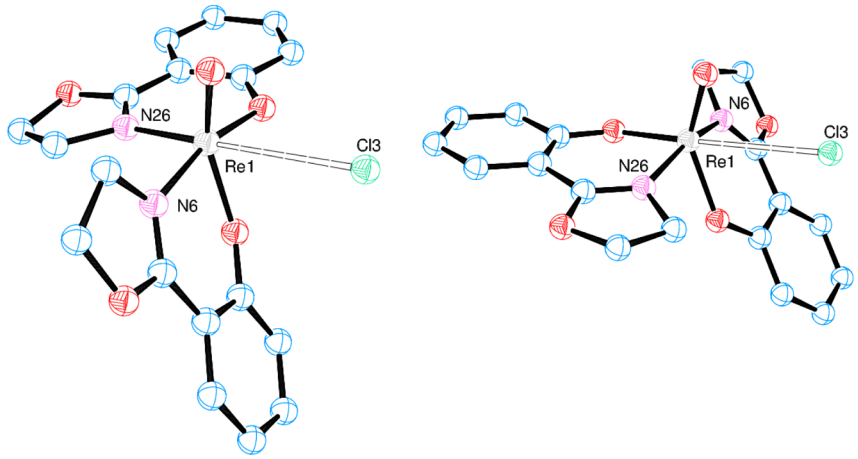

Figure 6. Calculated transition state structures {**3a-TS1**} and {**3a′-TS1**} for chloride abstraction.

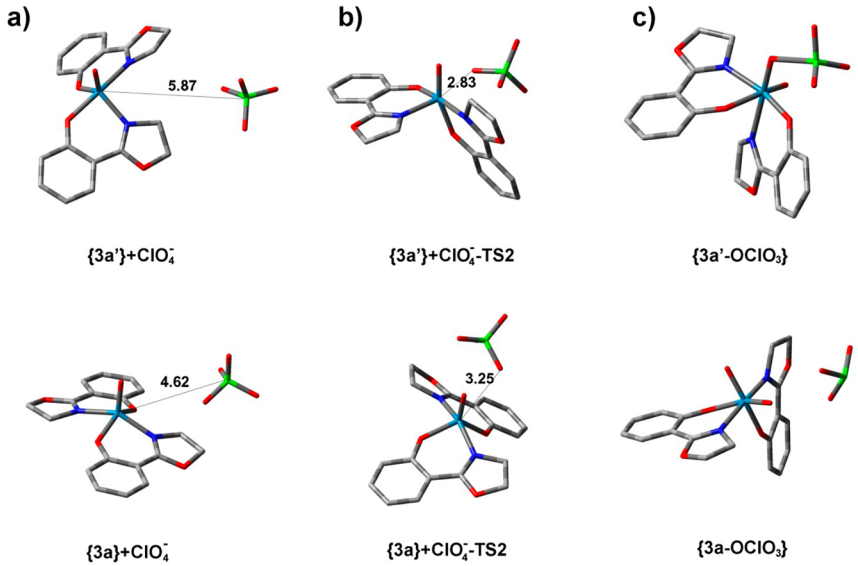

Figure 7. DFT modeling of perchlorate reduction: (a) approach of the perchlorate anion toward the cationic complexes {**3a**}$^+$ and {**3a′**}$^+$; (b) transition state structures; (c) products of reduction. The numbers indicate the calculated interatomic distances [Å].

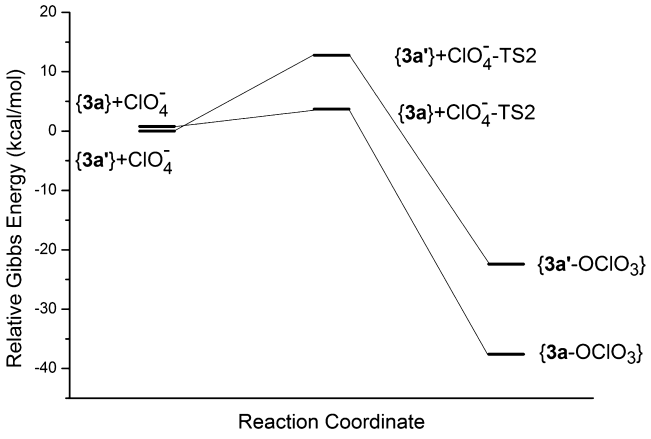

Figure 8. Relative Gibbs free energies of the RDS of perchlorate reduction.

the reduced catalytic activity, the oxidation of these complexes was followed by UV−vis spectroscopy. The oxidation reaction of the rhenium complexes with excess amounts of perchlorate without the presence of the O acceptor sulfide was investigated in order to ensure pseudo-first-order oxidations, allowing extraction of pseudo-first-order rate constants.

Kinetic experiments were conducted in CH_3CN/H_2O (95:5, v/v) at 20 °C. The increase in absorbance due to formation of the red dioxo species was monitored at 500 nm, as previously reported.[9] As shown in Figure 9, the rate of oxidation at lower perchlorate concentrations (up to 3×10^{-3} mol/L is identical for **3a** and [**3a′**](OTf). Thereafter, **3a** shows significantly higher rates, which is consistent with the observed higher catalytic activity in perchlorate reduction. Catalyst **3a′** revealed slower rate constants throughout the investigated perchlorate concentration window. In all cases, saturation in the rate was observed for increasing perchlorate concentrations. At saturation, k_{max} was determined via least-squares fitting.

Table 4 summarizes the data of the observed rates k_{max} for oxidation with perchlorate. The *N*,*N*-trans isomer **3a** shows approximately a 4 times higher rate than that of the *N*,*N*-cis complex **3a′**. The measured rate constants for **3a′** are quite similar regardless of the precatalyst used (**3a′** or the cationic complex [**3a′**](OTf)), hinting at formation of the same dioxo species after oxidation.

dx.doi.org/10.1021/ic501932c | *Inorg. Chem.* 2014, 53, 12918−12928

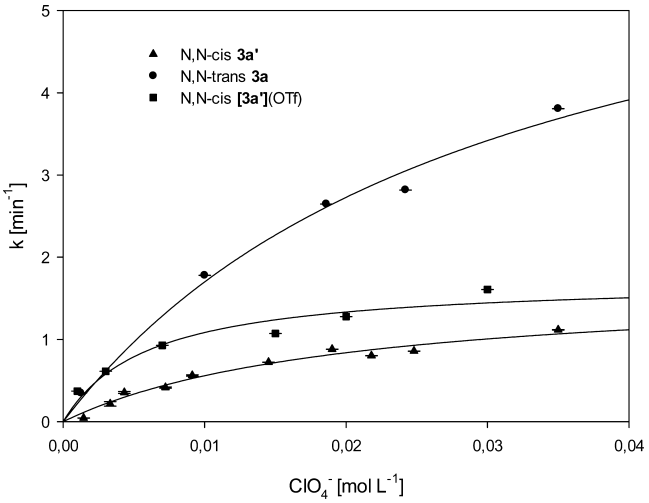

Figure 9. Comparison of the rates of oxidation for rhenium(V) catalysts by $LiClO_4$ for **3a** and [**3a′**](OTf) and by $AgClO_4$ for **3a′** depending on the perchlorate concentration.

Table 4. Observed Rate Constants k_{max} at Perchlorate Saturation

	k_{max} [min^{-1}]
3a	6.92 ± 1.25
3a′	1.67 ± 0.20
[**3a′**](OTf)	1.73 ± 0.20

CONCLUSIONS

The reduction of perchlorate ions under catalytic conditions of a set of oxorhenium(V) complexes was investigated. We were able to isolate and fully characterize two coordination isomers **3a** (*N*,*N*-trans) and **3a′** (*N*,*N*-cis), which showed a significant difference in the catalytic activity. Whereas with the previously published complex **3a**, 87% conversion of perchlorate was observed, with **3a′** only 16% perchlorate conversion was observed under the same conditions. Upon abstraction of the chloride ligand in **3a′** with Ag(OTf) to generate the cationic complex [**3a′**](OTf), perchlorate conversion significantly increases from 16 to 57%. Also, using $AgClO_4$ instead of $LiClO_4$ as the substrate led to an increase of conversion to 40%. Kinetic investigation by UV−vis spectroscopy showed that the rate of oxidation in the absence of sulfide is slower by a factor of ∼4 for *N*,*N*-cis complexes **3a′** and [**3a′**](OTf). In addition, the energy for chloride abstraction from **3a** and **3a′** was calculated and found to be 3.7 kcal/mol higher for **3a′** than for **3a**. Cleavage of the Cl−O bond in perchlorate was found to be the RDS and is for the *N*,*N*-trans isomer {**3a**}+ClO_4-TS2 energetically favored by 9.9 kcal/mol over the *N*,*N*-cis isomer {**3a′**}+ClO_4-TS2. Furthermore, all calculated optimized structures remain in their respective *N*,*N*-trans or *N*,*N*-cis configuration during the catalytic cycle. With these data at hand, we conclude that no isomerization, as previously suggested, occurs throughout the catalytic cycle. The neutral oxazoline N donor in the position trans to the Cl atom in **3a′** exhibits a lower trans effect compared to the anionic phenolate O atom in **3a**. This influences the kinetics in all steps of the catalytic cycle. This is supported by our observation that prior chloride abstraction from **3a′** leads to a more active catalyst but remains less active than **3a**. Thus, for efficient perchlorate reduction, an arrangement displaying a *trans*-X−Re−Cl unit, with X being a strong ligand such as a phenoxide, and a ligand environment that does not promote isomerization during catalysis are required.

EXPERIMENTAL SECTION

General Procedures. ***Caution!*** *Perchlorate salts of complexes with organic ligands are potentially explosive. Personal safety equipment has to be worn at all times when handling perchlorate salts in OAT reactions.* The rhenium precursors $[ReOCl_3(PPh_3)_2]$,[19,43] $[ReOCl_3(OPPh_3)(SMe_2)]$,[23] and $(NBu_4)[ReOCl_4]$[44] were prepared according to a previously published method. The Hoz ligand **1a** was prepared via a published route.[17] Chemicals were purchased from commercial sources and used without further purification. NMR spectra were recorded with a Bruker (300 MHz) instrument. Chemical shifts are given in ppm and are referenced to residual protons in the solvent. Coupling constants (*J*) are given in hertz (Hz). For complexes **2b** and **3a′**, no meaningful ^{13}C NMR spectra could be obtained because of low solubility. Data obtained from HSQC experiments are given instead. Mass spectrometry (MS) spectra were recorded with an Agilent 5973 MSD direct probe using the electron ionization (EI) technique. Samples for IR spectroscopy were measured on a Bruker Optics Alpha FT-IR spectrometer equipped with an ATR diamond probe head. Elemental analyses were carried out using a Heraeus Vario Elementar automatic analyzer at the Department of Inorganic Chemistry, Technical University Graz.

X-ray Crystal Structure Analysis. Structure determination of complexes **2a**, **3a**, **3a′**, and **4** via X-ray diffraction analysis has been performed on a Bruker-AXS Smart Apex CCD diffractometer. All measurements were performed using graphite-monochromatized Mo Kα radiation at 100 K. The structures were solved by direct methods (*SHELXS-97*)[45] and refined by full-matrix least-squares techniques against F^2 (*SHELXL-97*).[45] The H atoms of the CH_2 groups were refined with common isotropic displacement parameters for the H atoms of the same group and idealized geometry with approximately tetrahedral angles and C−H distances of 0.99 Å. The H atoms of the phenyl rings were put at the external bisectors of the C−C−C angles at C−H distances of 0.95 Å and common isotropic displacement parameters were refined for the H atoms of the same phenyl group. Crystallographic data (excluding structure factors) for **2a**, **3a**, **3a′**, and **4** were deposited with the Cambridge Crystallographic Data Centre as supplementary publication nos. 935350 (**2a**), 935351 (**3a**), 935352 (**3a′**), and 935353 (**4**). Copies of the data can be obtained free of charge upon application to The Director, CCDC, 12 Union Road, Cambridge CB2 1EZ, U.K. [fax (int.) +44-1223/336-033; e-mail deposit@ccdc.cam.ac.uk].

Computational Details. Calculations were performed at the DFT level of theory using the restricted Becke's three-parameter hybrid method with the Lee−Yang−Parr exchange-correlation functional (denoted as B3LYP).[34−36] The geometries of the complexes were calculated without symmetry constraint with the 6-31G basis set for H atoms and the 6-31+G(d) basis set for C, O, N, and Cl atoms.[46] An ECP LANL2DZ basis set was used for the Re center.[37−39] The chosen DFT functional and basis sets proved to give satisfactory results in computing other rhenium complexes as far as the structures and vibrational energies are concerned.[27,32,40−42] Frequency computations at the same level of theory were used to characterize the obtained stationary points. The absence of imaginary frequencies corresponded to minima, while only one imaginary frequency confirmed the existence of the transition state structures. All reported energies are Gibbs free energies (ΔG) in kcal/mol calculated for 298.15 K. All calculations were performed with the *Gaussian 09* package.[47]

Alternative One-Pot Synthesis of 1b. A mixture of ethyl salicylic ester (4.98 g, 30 mmol) and 2-amino-2-methylpropan-1-ol (2.67 g, 30 mmol) was heated to 170 °C for 16 h with a Dean−Stark trap to remove the liberated ethanol. Ligand **1b** forms in quantitative yield, albeit in lowered purity (85−90%), with the starting material salicylic ester being the main impurity. This material can be used as is in the synthesis of complexes **2b** and **3b** or further purified by vacuum distillation as described previously.[15]

dx.doi.org/10.1021/ic501932c | *Inorg. Chem.* 2014, 53, 12918−12928

Synthesis of [ReOCl$_2$(oz)(PPh$_3$)] (2a). [ReOCl$_2$(PPh$_3$)$_2$] (0.832 g, 1 mmol) and ligand **1a** (0.163 g, 1 mmol) were mixed in acetonitrile (40 mL) and refluxed for 2 h. The light-green solution obtained was concentrated to give a deep-green precipitate, which was collected by filtration, washed with acetonitrile, and dried in vacuo to give **2a**. Yield: 0.45 g (0.64 mmol, 64%). Light-green crystals suitable for single-crystal X-ray diffraction analysis were obtained by slow evaporation of an acetonitrile solution at room temperature. ^{1}H NMR (300 MHz, chloroform-*d*): δ 7.66−7.30 (m, 15H, Ar PPh$_3$), 7.31 (dd, J = 7.9 and 1.8 Hz, 1H, Ar oz), 7.06−6.97 (m, 1H, Ar oz), 6.84 (t, J = 7.3 Hz, 1H, Ar oz), 6.52 (d, J = 8.2 Hz, 1H, Ar oz), 4.71 (dt, J = 10.5 and 7.7 Hz, 1H, CH$_2$ oz), 4.39−4.09 (m, 2H, CH$_2$ oz), 3.32 (ddd, J = 13.2, 10.3, and 7.3 Hz, 1H, CH$_2$ oz). ^{13}C NMR (75 MHz, chloroform-*d*): δ 165.84, 161.78, 136.92, 134.22, 134.09, 131.51, 131.48, 131.11, 130.43, 130.33, 128.80, 128.66, 119.11, 109.47, 100.10, 67.69, 58.70. ^{31}P NMR (121 MHz, chloroform-*d*): δ −18.15. IR (ATR, cm^{-1}): 1624.64 ($\nu_{C=N}$), 963.06 ($\nu_{Re=O}$). EI-MS: m/z 434.9 [M$^+$ − PPh$_3$], 262.1 [PPh$_3$]. Anal. Calcd for C$_{27}$H$_{23}$Cl$_2$NO$_3$PRe (697.0): C, 46.49; H, 3.32; N, 2.01. Found: C, 45.88; H, 3.14; N, 2.17.

Synthesis of [ReOCl$_2$(dmoz)(PPh$_3$)] (2b). To a mixture of [ReOCl$_3$(PPh$_3$)$_2$] (0.832 g, 1 mmol) and ligand **1b** (0.246 g, 1 mmol) was added acetonitrile (40 mL), and the resulting solution was stirred under reflux for 2 h. The light-green solution obtained was concentrated, whereupon a deep-green precipitate formed. The latter was filtered, washed with acetonitrile, and dried in vacuo to give **2b**. Yield: 0.38 g (0.53 mmol, 52%). ^{1}H NMR (300 MHz, chloroform-*d*): δ 7.64 (dd, J = 7.8 and 1.9 Hz, 1H, Ar oz), 7.52−7.32 (m, 15H, Ar PPh$_3$), 7.02−6.88 (m, 1H, Ar oz), 6.92−6.85 (m, 1H, Ar oz), 6.20 (dd, J = 8.2 and 1.3 Hz, 1H, Ar oz), 4.42 (d, J = 8.2 Hz, 1H, CH$_2$ oz), 4.09 (d, J = 8.2 Hz, 1H, CH$_2$ oz), 1.80 (s, 3H, Me), 0.55 (s, 3H, Me). ^{13}C NMR (HSQC, chloroform-*d*): δ 131.16, 130.56, 134.36−128.57 (PPh$_3$), 119.32, 119.27, 79.05, 29.09, 25.35 (seven quaternary C atoms are not detected). ^{31}P NMR (121 MHz, chloroform-*d*): δ −18.7. IR (ATR, cm^{-1}): 1609.38 ($\nu_{C=N}$), 969.21 ($\nu_{Re=O}$). EI-MS: m/z 725.4 [M$^+$], 463.1 [M$^+$ − PPh$_3$], 262.1 [PPh$_3$]. Anal. Calcd for C$_{29}$H$_{27}$Cl$_2$NO$_3$PRe (725.62): C, 48.00; H, 3.75; N, 1.93. Found: C, 48.05; H, 3.70; N, 1.85.

Isolation of *N,N-cis*-[ReOCl(oz)$_2$] (3a′). *N,N*-Cis isomer **3a′** forms together with the previously published *N,N*-trans isomer **3a**.[9] The analytically pure material of the *N,N*-cis complex **3a′** is most conveniently isolated from the supernatant after filtration of **3a**, which precipitates first. The solvent EtOH is removed in vacuo, and the remaining crude material is then continuously extracted with Et$_2$O in a Soxhlet extractor. Yield (based on published procedure for *N,N*-trans isomer **3a**): 0.18 g (0.32 mmol, 40%). ^{1}H NMR (300 MHz, chloroform-*d*): δ 7.81 (dd, J = 8.1 and 1.8 Hz, 1H, Ar oz), 7.58 (ddd, J = 8.6, 6.3, and 1.8 Hz, 2H, Ar oz), 7.50−7.43 (m, 1H, Ar oz), 7.19 (ddd, J = 8.6, 7.2, and 1.8 Hz, 1H, Ar oz), 6.99−6.83 (m, 2H, Ar oz), 6.73 (dd, J = 8.2 and 0.7 Hz, 1H, Ar oz), 5.02 (dt, J = 10.8 and 8.3 Hz, 1H, CH$_2$ oz), 4.87 (q, J = 9.4 Hz, 1H, CH$_2$ oz), 4.69−4.36 (m, 3H, CH$_2$ oz), 4.19−3.95 (m, 2H, CH$_2$ oz), 3.71 (ddd, J = 12.3, 10.8, and 8.3 Hz, 1H, CH$_2$ oz). ^{13}C NMR (HSQC, chloroform-*d*): δ 137.47, 132.11, 129.85, 128.40, 123.47, 117.57, 119.72, 68.81, 68.12, 61.69, 61.66, 59.58 (six quaternary C atoms are not detected). IR (ATR, cm^{-1}): 1619.87 ($\nu_{C=N}$), 956.83 ($\nu_{Re=O}$). UV [CH$_3$CN/H$_2$O (95/5, v/v); λ_{max}, nm (ε, M^{-1} cm^{-1})]: 641 (96). Anal. Calcd for C$_{18}$H$_{16}$ClN$_2$O$_5$Re (561.99): C, 38.47; H, 2.78; N, 4.98. Found: C, 38.19; H, 2.85; N, 4.95.

Synthesis of *N,N-cis*-[ReO(oz)$_2$](SO$_3$CF$_3$) [3a′](OTf). Complex **3a′** (16.4 mg, 29 μmol, 1 equiv) was dissolved in 2 mL of CH$_3$CN, and 8.9 mg of Ag(OTf) (35 μmol, 1.2 equiv) was added. The solution turned dark green, and immediate precipitation of AgCl occurred. After filtration and removal of the solvent, analytically pure [**3a′**](OTf) was obtained as a dark-green solid. Yield: 16.9 mg (25 μmol, 86%). ^{1}H NMR (300 MHz, acetonitrile-d_3): δ 7.96 (dd, J = 8.1 and 1.8 Hz, 1H, Ar oz), 7.82 (dd, J = 7.9 and 1.8 Hz, 1H, Ar oz), 7.71 (ddd, J = 8.7, 7.1, and 1.8 Hz, 1H, Ar oz), 7.45 (ddd, J = 8.7, 7.4, and 1.8 Hz, 1H, Ar oz), 7.20 (ddd, J = 8.7, 5.6, and 1.2 Hz, 2H, Ar oz), 7.09−7.00 (m, 1H, Ar oz), 6.88 (dd, J = 8.4 and 1.0 Hz, 1H, Ar oz), 5.00 (m, 2H, CH$_2$ oz), 4.80 (t, J = 9.6 Hz, 2H, CH$_2$ oz), 4.42−4.03 (m, 3H, CH$_2$ oz), 3.92 (dt, J = 12.1 and 9.6 Hz, 1H, CH$_2$ oz). ^{13}C NMR (75 MHz, acetonitrile-d_3): δ 138.88, 138.16, 132.02, 131.52, 122.41, 121.21, 121.11, 119.52, 72.09, 69.77, 61.04, 60.34 (two quaternary C atoms obscured because of low solubility). ^{19}F NMR (282 MHz, acetonitrile-d_3): δ −79.34. IR (ATR, cm^{-1}): 1605.84, 1580.11 (s, $\nu_{C=N}$), 1223.30 (vs), 1025.20 (s), 633.83 (s). EI-MS: m/z 527.2 [M$^+$ − SO$_3$CF$_3$]. UV [CH$_3$CN/H$_2$O (95:5, v/v); λ_{max}, nm (ε, M^{-1} cm^{-1})]: 582 (200).

Synthesis of [ReOCl(dmoz)$_2$] (3b). (NBu$_4$)[ReOCl$_4$] (0.293 g, 0.5 mmol) in MeOH (20 mL) was slowly added to a colorless solution of sodium 2-(4,4-dimethyl-4,5-dihydrooxazol-2-yl)phenolate (0.213 g, 1 mmol) in MeOH (5 mL) under vigorous stirring, resulting in a dark-brown solution, which was refluxed for 4 h. Slow evaporation of the solvent over the course of 1 week at room temperature resulted in a green-brown suspension. The brown supernatant was filtered off, and the residual precipitate was washed three times with 5 mL of MeOH. The solid was recrystallized from dichloromethane to give blocks of dark-green crystals suitable for single-crystal X-ray diffraction analysis, which were filtered, washed with methanol, and dried in vacuo. Yield: 0.034 g (11.7%). ^{1}H NMR (300 MHz, chloroform-*d*): δ 7.95 (dd, J = 8.2 and 1.8 Hz, 1H, Ar oz), 7.74 (dd, J = 8.0 and 1.8 Hz, 1H, Ar oz), 7.40 (ddd, J = 8.7, 7.0, and 1.8 Hz, 1H, Ar oz), 7.21 (ddd, J = 8.3, 7.2, and 1.8 Hz, 1H, Ar oz), 6.93 (t, J = 7.3 Hz, 1H, Ar oz), 6.83 (d, J = 8.4 Hz, 1H, Ar oz), 6.80−6.71 (m, 2H, Ar oz), 4.70−4.48 (m, 4H, CH$_2$ oz), 1.96 (s, 3H, Me), 1.94 (s, 3H, Me), 1.85 (s, 3H, Me), 1.65 (s, 3H, Me). ^{13}C NMR (75 MHz, chloroform-*d*): δ 178.32, 169.78, 166.75, 165.00, 136.06, 135.96, 131.00, 130.54, 121.00, 119.47, 118.69, 118.04, 110.66, 110.50, 82.12, 79.58, 79.09, 73.05, 27.65, 27.39, 27.20, 26.06. IR: (ATR, cm^{-1}): 1604.03 ($\nu_{C=N}$), 954.83 ($\nu_{Re=O}$). EI-MS: m/z 618.09 [M$^+$]. Anal. Calcd for C$_{22}$H$_{24}$ClN$_2$O$_5$Re (618.09): C, 42.75; H, 3.91; N, 4.53. Found: C, 42.62; H, 3.72; N, 4.33.

Synthesis of [ReO(OMe)(dmoz)$_2$] (4). To 200 mg (0.32 mmol) of **3b** dissolved in MeOH (20 mL) was added NaOMe (21 mg, 0.39 mmol), and the resulting solution was refluxed. The reaction mixture was stirred under reflux for 1 h. The initially deep-green solution turned blue-green. Upon cooling and concentration, **4** precipitated as a dark-green crystalline material. Yield: 158 mg (0.25 mmol, 79%). ^{1}H NMR (300 MHz, chloroform-*d*): δ 7.85 (d, J = 8.2 Hz, 2H, Ar oz), 7.37 (t, J = 7.8 Hz, 2H, Ar oz), 7.02 (d, J = 8.5 Hz, 2H, Ar oz), 6.68 (t, J = 7.5 Hz, 2H, Ar oz), 4.41 (s, 4H, CH$_2$ oz), 3.37 (s, 3H, OMe), 1.84 (s, 6H, Me), 1.82 (s, 6H, Me). ^{13}C NMR (75 MHz, chloroform-*d*): δ 176.61, 167.65, 135.03, 130.36, 121.68, 117.16, 110.12, 110.32, 81.16, 74.21, 57.26, 27.34. EI-MS: m/z 614.3 [M$^+$]. Anal. Calcd for C$_{23}$H$_{27}$N$_2$O$_6$Re (613.68): C, 45.01; H, 4.43; N, 4.56. Found: C, 44.62; H, 4.72; N, 4.33.

■ ASSOCIATED CONTENT

Supporting Information

X-ray crystallographic data in CIF format, comparisons of ^{1}H NMR spectra of **3a** and **3a′** (Figure S1) and of **3a**, **3a′**, and **3b** (Figure S2), tables including measured and calculated bond lengths (Table S1), natural population analysis of the dissociation of Cl from **3a** and **3a′** (Tables S2 and S3), discussion of the solid-state structure of **3a**, full details on crystallographic data acquisition as well as data refinement for **2a**, **3a**, **3a′**, and **4**, and calculated geometries and relative potential energies for perchlorate reduction. This material is available free of charge via the Internet at http://pubs.acs.org.

■ AUTHOR INFORMATION

Corresponding Author

*E-mail: nadia.moesch@uni-graz.at.

Present Address

‡B.T.: Department of Chemistry, Addis Ababa University, Queen Elisabeth II Street, Addis Ababa, Ethiopia.

Notes

The authors declare no competing financial interest.

■ ACKNOWLEDGMENTS

The authors gratefully acknowledge support from NAWI Graz. B.T. thanks Kotebe University College, Addis Ababa, Ethiopia, for financial support of his Ph.D. program.

■ REFERENCES

(1) Brown, G. M.; Gu, B. In *Perchlorate*; Gu, B., Coates, J. D., Eds.; Kluwer Academic Publishers: Boston, 2006; pp 17−47.
(2) Mahmudov, R.; Shu, Y.; Rykov, S.; Chen, J.; Huang, C. P. *Appl. Catal., B* **2008**, *81*, 78−87.
(3) Srinivasan, R.; Sorial, G. A. *Sep. Purif. Technol.* **2009**, *69*, 7−21.
(4) (a) Earley, J. E.; Kallen, T. W. *Inorg. Chem.* **1971**, *10*, 1152−1155. (b) Taube, H. In *Mechanistic aspects of inorganic reactions*; Endicott, J. F., Rorabacher, D. B., Eds.; American Chemical Society: Washington, DC, 1982; Vol. *198*; pp 151−171. (c) Espenson, J. H. In *Perchlorate in the Environment*; Urbansky, E. T., Ed.; Springer: Boston, MA, 2000; pp 1−7.
(5) (a) Ye, L.; You, H.; Yao, J.; Su, H. *Desalination* **2012**, *298*, 1−12. (b) Hatzinger, P. B. *Environ. Sci. Technol.* **2005**, *39*, 239A.
(6) Wang, C.; Huang, Z.; Lippincott, L.; Meng, X. *J. Hazard. Mater.* **2010**, *175*, 159−164.
(7) Haight, G. P.; Sager, W. F. *J. Am. Chem. Soc.* **1952**, *74*, 6056−6059.
(8) (a) Abu-Omar, M. M.; Espenson, J. H. *Inorg. Chem.* **1995**, *34*, 6239−6240. (b) Abu-Omar, M. M.; Appelman, E. H.; Espenson, J. H. *Inorg. Chem.* **1996**, *35*, 7751−7757.
(9) Abu-Omar, M. M.; McPherson, L. D.; Arias, J.; Béreau, V. M. *Angew. Chem., Int. Ed.* **2000**, *39*, 4310−4313.
(10) (a) Hurley, K. D.; Shapley, J. R. *Environ. Sci. Technol.* **2007**, *41*, 2044−2049. (b) Hurley, K. D.; Zhang, Y.; Shapley, J. R. *J. Am. Chem. Soc.* **2009**, *131*, 14172−14173. (c) Zhang, Y.; Hurley, K. D.; Shapley, J. R. *Inorg. Chem.* **2011**, *50*, 1534−1543.
(11) Arias, J.; Newlands, C. R.; Abu-Omar, M. M. *Inorg. Chem.* **2001**, *40*, 2185−2192.
(12) Abu-Omar, M. M. *Chem. Commun.* **2003**, 2102.
(13) Abu-Omar, M. M. *Comments Inorg. Chem.* **2003**, *24*, 15−37.
(14) McPherson, L. D.; Drees, M.; Khan, S. I.; Strassner, T.; Abu-Omar, M. M. *Inorg. Chem.* **2004**, *43*, 4036−4050.
(15) Cozzi, P. G.; Floriani, C.; Chiesi-Villa, A.; Rizzoli, C. *Inorg. Chem.* **1995**, *34*, 2921−2930.
(16) Black, D. S.; Wade, M. J. *Aust. J. Chem.* **1972**, *25*, 1797−1810.
(17) Hoveyda, H. R.; Karunaratne, V.; Rettig, S. J.; Orvig, C. *Inorg. Chem.* **1992**, *31*, 5408−5416.
(18) Traar, P.; Schachner, J. A.; Steiner, L.; Sachse, A.; Volpe, M.; Mösch-Zanetti, N. C. *Inorg. Chem.* **2011**, *50*, 1983−1990.
(19) Grove, D. E.; Wilkinson, G. *J. Chem. Soc. A* **1966**, 1224−1230.
(20) Machura, B.; Wolff, M.; Gryca, I. *Coord. Chem. Rev.* **2014**, *275*, 154−164.
(21) Lobmaier, G. M.; Frey, G. D.; Dewhurst, R. D.; Herdtweck, E.; Herrmann, W. A. *Organometallics* **2007**, *26*, 6290−6299.
(22) Machura, B.; Wolff, M.; Benoist, E.; Schachner, J. A.; Mösch-Zanetti, N. C. *Dalton Trans.* **2013**, *42*, 8827.
(23) Sherry, B. D.; Loy, R. N.; Toste, F. D. *J. Am. Chem. Soc.* **2004**, *126*, 4510−4511.
(24) Schwade, V. D.; Hagenbach, A.; Schulz Lang, E.; Klauke, K.; Mohr, F.; Abram, U. *Eur. J. Inorg. Chem.* **2014**, *2014*, 1949−1954.
(25) (a) Mazzi, U.; Refosco, F.; Bandoli, G.; Nicolini, M. *Transition Met. Chem.* **1985**, *10*, 121−127. (b) Banbery, H. J.; Hussain, W.; Hamor, T. A.; Jones, C. J.; McCleverty, J. A. *Dalton Trans.* **1990**, 657−661.
(26) (a) Sachse, A.; Mösch-Zanetti, N. C.; Lyashenko, G.; Wielandt, J. W.; Most, K.; Magull, J.; Dall'Antonia, F.; Pal, A.; Herbst-Irmer, R. *Inorg. Chem.* **2007**, *46*, 7129−7135. (b) Machura, B.; Kusz, J. *Polyhedron* **2008**, *27*, 923−932. (c) Fernandes, A. G.; Maia, P. I.; Souza, E. J. de; Lemos, S. S.; Batista, A. A.; Abram, U.; Ellena, J.; Castellano, E. E.; Deflon, V. M. *Polyhedron* **2008**, *27*, 2983−2989.
(27) Machura, B.; Kruszynski, R.; Kusz, J. *Polyhedron* **2008**, *27*, 1679−1689.
(28) Schröckeneder, A.; Traar, P.; Raber, G.; Baumgartner, J.; Belaj, F.; Mösch-Zanetti, N. C. *Inorg. Chem.* **2009**, *48*, 11608−11614.
(29) Machura, B.; Wolff, M.; Tabak, D.; Schachner, J. A.; Mösch-Zanetti, N. C. *Eur. J. Inorg. Chem.* **2012**, 3764−3773.
(30) Lin, A.; Peng, H.; Abdukader, A.; Zhu, C. *Eur. J. Org. Chem.* **2013**, *2013*, 7286−7290.
(31) Shuter, E.; Hoveyda, H. R.; Karunaratne, V.; Rettig, S. J.; Orvig, C. *Inorg. Chem.* **1996**, *35*, 368−372.
(32) Travia, N. E.; Xu, Z.; Keith, J. M.; Ison, E. A.; Fanwick, P. E.; Hall, M. B.; Abu-Omar, M. M. *Inorg. Chem.* **2011**, *50*, 10505−10514.
(33) Barandov, A.; Abram, U. *Z. Anorg. Allg. Chem.* **2007**, *633*, 1897−1899.
(34) Becke, A. D. *Phys. Rev. A* **1988**, *38*, 3098−3100.
(35) Becke, A. D. *J. Chem. Phys.* **1993**, *98*, 1372−1377.
(36) Becke, A. D. *J. Chem. Phys.* **1993**, *98*, 5648−5652.
(37) Hay, P. J.; Wadt, W. R. *J. Chem. Phys.* **1985**, *82*, 299−310.
(38) Hay, P. J.; Wadt, W. R. *J. Chem. Phys.* **1985**, *82*, 270−283.
(39) Wadt, W. R.; Hay, P. J. *J. Chem. Phys.* **1985**, *82*, 284−298.
(40) Yang, X.; Hall, M. B. *J. Am. Chem. Soc.* **2007**, *129*, 1560−1567.
(41) Gryca, I.; Machura, B.; Małecki, J. G.; Shul'pina, L. S.; Pombeiro, A. J. L.; Shul'pin, G. B. *Dalton Trans.* **2014**, *43*, 5759.
(42) Huber, S.; Pöthig, A.; Herrmann, W. A.; Kühn, F. E. *J. Organomet. Chem.* **2014**, *760*, 156−160.
(43) Chatt, J.; Rowe, G. A. *J. Chem. Soc.* **1962**, 4019.
(44) Alberto, R.; Schibli, R.; Egli, A.; August Schubiger, P.; Herrmann, W. A.; Artus, G. R. J.; Abram, U.; Kaden, T. A. *J. Organomet. Chem.* **1995**, *493*, 119−127.
(45) Sheldrick, G. M. *Acta Crystallogr., Sect. A: Found. Crystallogr.* **2008**, *64*, 112−122.
(46) Schäfer, A.; Horn, H.; Ahlrichs, R. *J. Chem. Phys.* **1992**, *97*, 2571−2577.
(47) Frisch, M. J.; Trucks, G. W.; Schlegel, H. B.; Scuseria, G. E.; Robb, M. A.; Cheeseman, J. R.; Scalmani, G.; Barone, V.; Mennucci, B.; Petersson, G. A.; Nakatsuji, H.; Caricato, M.; Li, X.; Hratchian, H. P.; Izmaylov, A. F.; Bloino, J.; Zheng, G.; Sonnenberg, J. L.; Hada, M.; Ehara, M.; Toyota, K.; Fukuda, R.; Hasegawa, J.; Ishida, M.; Nakajima, T.; Honda, Y.; Kitao, O.; Nakai, H.; Vreven, T.; Peralta, J. E.; Ogliaro, F.; Bearpark, M.; Heyd, J. J.; Brothers, E.; Kudin, K. N.; Staroverov, V. N.; Kobayashi, R.; Normand, J.; Raghavachari, K.; Rendell, A.; Burant, J. C.; Iyengar, S. S.; Tomasi, J.; Cossi, M.; Rega, N.; Millam, J. M.; Klene, M.; Knox, J. E.; Cross, J. B.; Bakken, V.; Adamo, C.; Jaramillo, J.; Gomperts, R.; Stratmann, R. E.; Yazyev, O.; Austin, A. J.; Cammi, R.; Pomelli, C.; Ochterski, J. W.; Martin, R. L.; Morokuma, K.; Zakrzewski, V. G.; Voth, G. A.; Salvador, P.; Dannenberg, J. J.; Dapprich, S.; Daniels, A. D.; Farkas; Foresman, J. B.; Ortiz, J. V.; Cioslowski, J.; Fox, D. J. *Gaussian 09*, revision A.02; Gaussian Inc.: Wallingford, CT, 2009.